Symmetry Locking and Commensurate Vortex Domain Formation in Periodic Pinning Arrays

A. N. Grigorenko* and S. J. Bending

Department of Physics, University of Bath, Claverton Down, Bath BA2 7AY, United Kingdom

M. J. Van Bael, M. Lange, and V. V. Moshchalkov

Laboratorium voor Vaste-Stoffysica en Magnetisme, Katholieke Universiteit Leuven, Celestijnenlaan 200D, 3001 Leuven, Belgium

H. Fangohr and P. A. J. de Groot

*School of Engineering Sciences & Department of Physics and Astronomy, University of Southampton,
Southampton SO17 1BJ, United Kingdom*

The spontaneous formation of *domains* of commensurate vortex patterns near rational fractional matching fields of a periodic pinning array has been investigated with high resolution scanning Hall probe microscopy. We show that domain formation is promoted due to the efficient incorporation of mismatched excess vortices and vacancies at the *corners* of domain walls, which outweighs the energetic cost of creating them. Molecular dynamics simulations with a generic pinning potential reveal that domains are formed only when vortex-vortex interactions are long range.

In many physical systems high symmetry ordering occurs only for certain specific values of the system parameters, and these transient symmetries are important for their excitation spectra. Nearby broken symmetry states frequently take the form of coexisting highly ordered domains separated by domain walls, and familiar examples include domains formed in ferromagnets, during crystal growth (e.g., twinning) and in liquid crystal films [1]. The same considerations apply to filling an ordered artificial array in a thin superconducting film with vortices, which is a problem that has recently received much attention with a view to enhancing the critical current of the film. In this case it is known that commensurate structures can be formed at certain specific values of the vortex density which give rise to sharp peaks in the bulk magnetization and critical current [2–8]. The existence of commensurate structures has been verified directly using Lorentz [9] and scanning Hall probe (SHPM) [10,11] microscopies. Theoretically the probability of observing these "pure" matching structures on a macroscopic scale is proportional to the measure of the parameter space at which they exist and, strictly speaking, is supposed to be zero when interactions can be neglected. This constraint is, however, relaxed for integer matching fields (when an integer number of flux quanta per unit cell is applied) due to magnetic "lock-in" phenomena when the local magnetic induction becomes fixed at the matching field over a finite applied field range. In this case lock-in can arise due to the formation of a "terraced" critical state whereby a staircase of one or more terraces of different integer matching fields exist with very high screening currents flowing at the sample edges and interterrace boundaries [12,13]. Weaker matching effects are observed near rational fractional matching fields, where molecular dynamics simulations predicted

[14] and imaging experiments confirmed [9] that ordered vortex structures form which are commensurate with the pinning array. One important feature that distinguishes fractional matching states from integer ones is that multiple possible degenerate structures exist under the symmetry transformations of the pinning array. Recent SHPM images have revealed the spontaneous formation of complex composite structures of degenerate domains separated by domain walls near rational fractional filling [10,11]. This phenomenon was entirely unanticipated since, in stark contrast to ferromagnetic materials, the energy density and magnetization of different domains are identical, and the driving force for domain formation and the estimation of typical domain sizes has, until now, remained an unsolved problem. We report a systematic study of the evolution of the domain structure with magnetic field and show that domain formation is a direct consequence of long-range vortex-vortex interactions which exist in thin superconducting films. *Corners in domain walls prove to be efficient "sinks" for fractions of unmatched excess vortices or vacancies, and allow commensurate states to exist over a broad range of applied magnetic fields.*

A variety of different artificial pinning strategies have been successfully employed including arrays of submicron holes (antidots) [2–4] or ferromagnetic dots with in-plane [5,6] and perpendicular anisotropy [7,8], and the qualitative features of both integer and fractional matching phenomena appear to be generic. Our imaging experiments were performed on a $t = 50$ nm thick granular Pb film ($T_c = 7.17$ K) deposited over an $a_0 = 1$ μm period square array ($H_1 = \Phi_0/a_0^2 = 20.67$ Oe) of 0.4 μm square ferromagnetic "dots" with perpendicular magnetic anisotropy patterned in a $[\mathrm{Co}(0.3\ \mathrm{nm})/\mathrm{Pt}(1.1\ \mathrm{nm})]_{10}$ multilayer film. The overall

array size was ~ 2 mm $\times 2$ mm (much bigger than any important length scale) and contained about 4×10^{6} magnetic dots. It exhibited rather square magnetization loops with large coercive fields (~ 1 kOe) allowing the imposition of magnetic templates which were stable at the low applied fields where matching effects were observed. A schematic diagram of the investigated sample is shown in the inset of Fig. 1 and further details of the sample preparation are given elsewhere [6,8,15]. The effective penetration depth of our Pb film at high temperatures when $\lambda(T) \gg t$ [16] was estimated from the upper critical field $H_{c2}(0)$ measured on a 25 nm reference Pb film and found to be $\Lambda(T) = 2\lambda^{2}(T)/t = 92$ nm$/(1 - T/T_{c})$. The SHPM used was able to generate maps of the local induction with ~ 0.4 μm spatial resolution and minimum detectable fields ~ 1 μT/Hz$^{0.5}$. A more detailed description is given in Ref. [17].

Figure 1(a) shows a "local" magnetization loop ($M_{\ell} = B_{\ell} - \mu_{0}H$) measured with the Hall probe stationary a few microns above the surface of our sample at $T = 6.9$ K ($T/T_{c} = 0.962$), after the pinning array had been magnetized to saturation in the down ($H < 0$) direction above T_{c}. Strongly asymmetric vortex pinning is observed due

to the fact that vortices whose fields are parallel to the Co/Pt dot magnetic moments ($H < 0$) are attracted to it and become strongly pinned, while those with antiparallel fields ($H > 0$) are repelled into interstitial spaces and are mobile [15]. For the parallel orientation ($H < 0$) clear matching peaks are seen at integer ($-1H_{1}, -2H_{1}$) and rational fractional ($-0.75H_{1}, -1.5H_{1}$) matching fields. Surprisingly, no clearly resolved structure is seen near $-0.5H_{1}$ or $-0.33H_{1}$ although, as we will show, commensurate structures definitely exist at these matching fields. The parallel plot of local magnetic induction [Fig. 1(b)] reveals lock-in phenomena at integer matching fields and $H = -0.75H_{1}$, where the slope becomes much shallower, but there is again no clear evidence for lock-in at other rational fractions.

High-resolution SHPM images were made of the vortex structures formed after field cooling to low temperatures. Figures 2(a)–2(e) show a typical family of images at fields close to $-H_{1}/2$. At exactly $H = -H_{1}/2$ [Fig. 2(d)] a very well ordered "checkerboard" structure is observed where every second pinning site is occupied by a vortex. Remarkably, cooling the sample at fields slightly above or below $-H_{1}/2$ did not result in excess vortices or vacancies in the commensurate lattice as is the case at field values close to integer matching. Instead coexisting domains of the two degenerate commensurate states (related by a translation of one lattice vector of the pinning array) are observed separated by domain walls of varying complexity. The latter appear to move smoothly as slightly different cooling fields are employed [cf. the
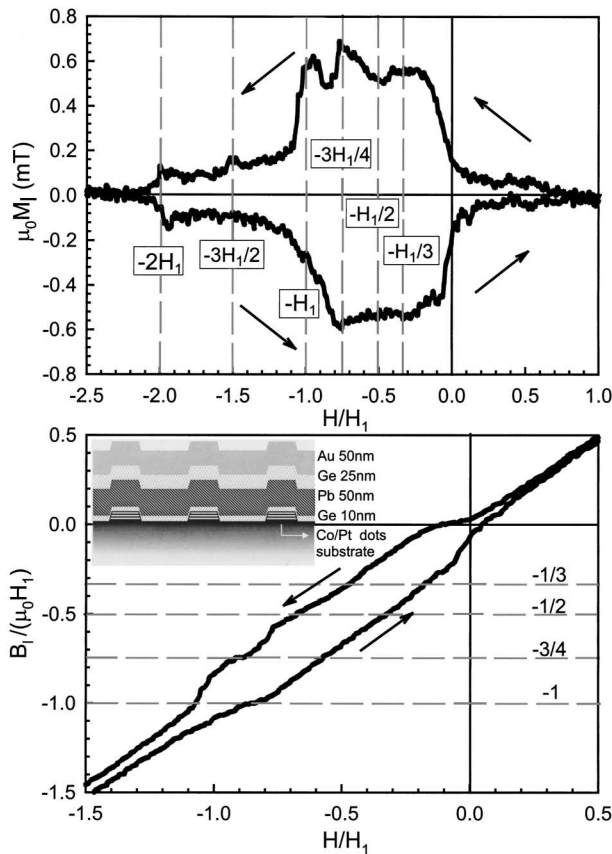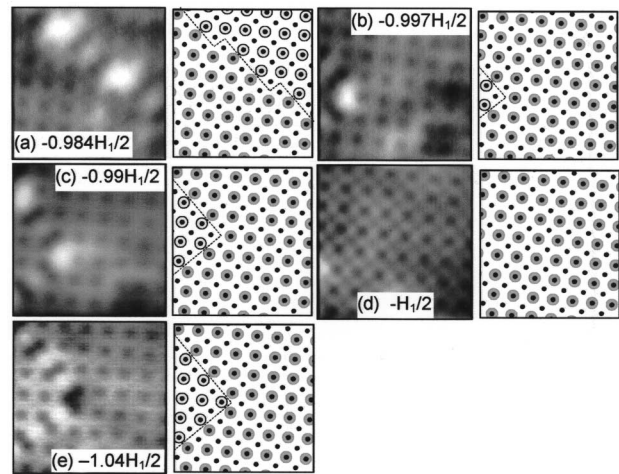

FIG. 1. Local magnetization (a) and magnetic induction (b) as a function of applied magnetic field at 6.9 K. Dashed lines indicate the expected location of matching features. Inset shows a schematic diagram of the pinning array.

FIG. 2. SHPM images of commensurate vortex configurations after field cooling close to the half-matching field. (a) $H = -0.984(H_{1}/2)$, $T = 5.5$ K [grayscale (GS) spans ~ 0.28 mT]. (b) $H = -0.997(H_{1}/2)$, $T = 5.5$ K (GS $\sim$ 0.24 mT). (c) $H = -0.990(H_{1}/2)$, $T = 5.5$ K (GS $\sim$ 0.27 mT). (d) The "checkerboard" configuration at $H = -H_{1}/2$, $T = 6.8$ K (GS ~ 0.20 mT). (e) $H = -1.04H_{1}/2$, $T = 6.0$ K (GS ~ 0.20 mT). The right-hand panels show clearer sketches of the domain structure in each adjacent image.

transition from Fig. 2(b) to Fig. 2(c)] and their presence does not seem to be related to the possible existence of inhomogeneities in the pinning array. There is a crucial difference between domain structures at fields slightly above and slightly below half matching. For $|H| < H_1/2$, when vacancies should exist in the checkerboard structure, the corners where domain walls bend by 90° comprise a "low density" square cluster of *three unoccupied pins and one occupied one*. In contrast, for $|H| > H_1/2$, when excess vortices should exist, the corners are composed of a "high density" cluster of *three occupied pins and one unoccupied one*. Hence, despite the increase in energy associated with the straight segments of domain wall, domain formation is favored because the incorporation of the mismatched vortices and vacancies into domain wall corners lowers the overall energy.

For a short-range vortex-vortex interaction one would expect the energy of the straight domain walls to be prohibitively large and the ground state should consist of "checkerboard-interstitials" or on-site "vacancies." However, in thin films at temperatures close to T_c, when $\lambda(T) \gg t$, Pearl [16] has shown that vortex-vortex interactions are long range, decaying as $\sim \log_e(\Lambda/r)$ for $r \ll \Lambda(T)$ and $\sim 1/r$ for $r \gg \Lambda(T)$, and domains can become favorable. Figures 3(a)–3(c) illustrate some possible domain structures. Simple "bookkeeping" reveals that the square domain in Fig. 3(a) with four high-density corners can accommodate exactly one excess vortex (i.e., $\Phi_0/4$ per corner). Translating the square domain one lattice site vertically (or horizontally) as shown in Fig. 3(b) generates a domain with low-density corners which can accommodate exactly one vacancy. Alternatively, stripelike domains could form as illustrated in Fig. 3(c) with either high- or low-density domain wall corners [cf. Fig. 2(a)].

To demonstrate that long-range vortex-vortex interactions promote domain formation, molecular dynamics simulations were performed with a generic pinning potential. Considering vortices as stiff massless lines, overdamped Langevin dynamics simulations of an effectively two-dimensional vortex system were carried out [18]. The long-range vortex-vortex interaction energy [$\lambda(T) \gg t$] was described by [16]

$$U^{vv}(r) = \frac{2\Phi_0^2 t}{4\pi\mu_0\lambda(T)^2}\left[H_0\left(\frac{r}{\Lambda}\right) - Y_0\left(\frac{r}{\Lambda}\right)\right], \qquad (1)$$

where $H_0(Y_0)$ is a Struve(Bessel) function of the second kind. The short-range vortex-vortex interaction energy, which is appropriate in thick films [$t \gg \lambda(T)$], was described by

$$U^{vv}(r) = \frac{2\Phi_0^2 t}{4\pi\mu_0\lambda(T)^2}K_0\left(\frac{r}{\lambda}\right), \qquad (2)$$

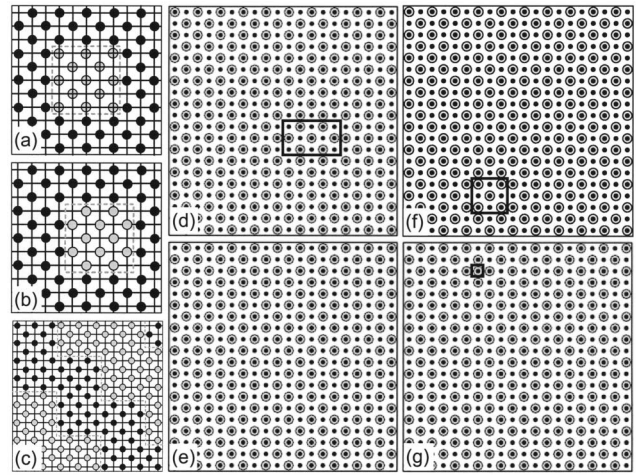where K_0 is the modified Bessel function of the second kind.

FIG. 3. Sketches of possible domain structures. Square domain accommodating (a) one excess vortex and (b) one vacancy. (c) Possible stripe domain structure. Molecular dynamics simulation results with a long-range vortex-vortex interaction for (d) half-matching field plus one vacancy, (e) half-matching field, and (f) half-matching field plus one excess vortex. (g) Same simulation as (f) but with a short-range vortex-vortex interaction.

The differential equation was solved numerically subject to periodic boundary conditions in order to compute the time progression of the system. Starting from a high temperature molten vortex configuration, we slowly annealed the system in the presence of a periodic pinning potential ($a_0 = 1 \ \mu$m) to zero temperature. The interaction of a vortex with each pinning site was assumed proportional to $-1/(\rho^2 + c)$ where ρ was the distance to the center of the pin, and c^{-1} a measure of the pin's depth. The results of the model did not depend sensitively on the details of the pinning potential. Figures 3(d) and 3(e) show typical results of the simulation for 400 pinning sites when the long-range interaction [Eq. (1)] with $\Lambda = 2 \ \mu$m was used in order to compare with the data of Fig. 1. For exactly half-matching conditions the checkerboard structure of Fig. 3(e) is reproduced. With one vacancy present, a rectangular domain with four low-density corners is created [Fig. 3(d)], while with one excess vortex a square domain with four high-density corners is found [Fig. 3(f)], in agreement with the images in Fig. 2. Figure 3(g) is a repeat of the calculation with one excess vortex for the short-range vortex-vortex potential [Eq. (2)] where we find, as expected, that the excess vortex is located at an unoccupied pin in the checkerboard lattice.

A simple "mean-field" analytic model of our system, where the flux associated with each lattice site is averaged over the four adjacent unit cells, confirms that Λ sets a characteristic length scale for the size of domains. Within this picture the domain walls vanish and the only long-range interactions are between the fractional flux quanta ($\Phi_0/4$) associated with the domain corners. Adding the
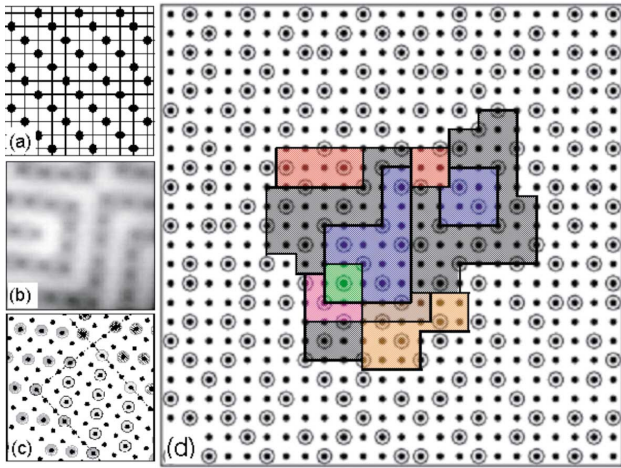
FIG. 4 (color online). (a) Sketch of expected commensurate structure at one-third matching. (b) SHPM image of commensurate vortex domains after field cooling at $H = -H_1/3$, $T = 5.5$ K (GS ~ 0.26 mT). (c) Clearer sketch of the domain structure in (b). (d) Molecular dynamics simulation result with a long-range vortex-vortex interaction for $H = -H_1/3$.

domain wall energy (σ per lattice site) and assuming $w > \Lambda > a_0$, the total energy associated with a domain of side length w is approximately $E(w) \sim 4\sigma w/a_0 + (4 + \sqrt{2})\Phi_0^2/(8\mu_0\pi^2 w)$. For typical sample parameters we calculate numerically that $\sigma \sim U^{vv}(a_0)/50 \sim \Phi_0^2/50\pi\mu_0\Lambda$ and the domain energy has a minimum at $w \sim 2\sqrt{a_0\Lambda}$. The effective penetration depth used in simulations $\Lambda = 2$ μm represents a much higher reduced temperature ($T/T_c \equiv 0.954$) than that corresponding to our field-cooled SHPM images. We assume, however, that the latter represent metastable states which become "frozen in" close to T_c where the penetration depth is much longer.

The checkerboard structure at $|H| = H_1/2$ preserves the fourfold rotational symmetry of the pinning array and appears rather robust with respect to the specific form of vortex-vortex interactions. This is not true of the structure at $|H| = H_1/3$ where the ground state was originally predicted to be one of six degenerate symmetry-breaking chain states as sketched in Fig. 4(a) [19]. These represent an inefficient way of packing vortices, and one might anticipate that a multidomain state would have lower energy, even *exactly* at the matching field [20]. The multidomain SHPM image at $|H| = H_1/3$ [Fig. 4(b)] shows this to be the case. This behavior is also confirmed in the simulation with the same long-range vortex-vortex potential as before. A typical simulation for 24×24 sites is illustrated in Fig. 4(d) and is a complex composite of all six degenerate chain structures (a few possible domain assignments have been sketched near the center).

In conclusion, we have shown that vortex domain formation near rational fractional matching is a consequence of domain wall topology and long-range vortex interactions in thin films at high temperatures. Domain corners incorporate fractions of excess vortices and vacancies and the overall energy is lowered because the system is able to lock to the symmetry of the pinning array within a domain, yet the magnetic induction averaged over several domains can vary around the exact matching field. This explains the absence of some fractional magnetization peaks even when matching occurs (see Fig. 1). Matching structures, which strongly break the symmetry of the pinning array, can even be unstable with respect to domain formation *exactly* at the matching field. The number of domains and domain sizes are generally governed by $\Lambda(T)$ (at which the domain structure becomes frozen), a_0, and the number of mismatched vortices.

*Current address: Department of Physics, University of Manchester, Manchester, United Kingdom.
[1] D. R. Link et al., Science **278**, 1924 (1997).
[2] A. F. Hebard, A. T. Fiory, and S. Somekh, Appl. Phys. Lett. **32**, 73 (1978).
[3] M. Baert et al., Phys. Rev. Lett. **74**, 3269 (1995).
[4] M. Baert et al., Europhys. Lett. **29**, 157 (1995).
[5] J. I. Martín et al., Phys. Rev. Lett. **79**, 1929 (1997).
[6] M. J. Van Bael et al., Phys. Rev. Lett. **86**, 155 (2001).
[7] D. J. Morgan and J. B. Ketterson, Phys. Rev. Lett. **80**, 3614 (1998).
[8] M. J. Van Bael et al., Physica (Amsterdam) **369C**, 97 (2002).
[9] K. Harada et al., Science **274**, 1167 (1996).
[10] S. B. Field et al., Phys. Rev. Lett. **88**, 067003 (2002).
[11] A. N. Grigorenko et al., Phys. Rev. B **63**, 052504 (2001).
[12] L. D. Cooley and A. M. Grishin, Phys. Rev. Lett. **74**, 2788 (1995).
[13] V. V. Moshchalkov et al., Phys. Rev. B **54**, 7385 (1996).
[14] C. Reichhardt et al., Phys. Rev. B **54**, 16 108 (1996).
[15] M. J. Van Bael et al. (to be published).
[16] J. Pearl, Appl. Phys. Lett. **5**, 65 (1964).
[17] A. Oral, S. J. Bending, and M. Henini, Appl. Phys. Lett. **69**, 1324 (1996).
[18] H. Fangohr, S. J. Cox, and P. A. J. de Groot, Phys. Rev. B **64**, 064505 (2001).
[19] G. I. Watson, Physica (Amsterdam) **246A**, 253 (1997).
[20] C. Reichhardt and N. Gronbech-Jensen, Phys. Rev. B **63**, 054510 (2001).